ЖЭТФ, 2015, том 148, вып. 6 (12), стр. 1115–1129

MUON ANOMALOUS MAGNETIC MOMENT IN THE SUPERSYMMETRIC ECONOMICAL 3-3-1 MODEL

***D. T. Binh*[*], *D. T. Huong*[**], *H. N. Long*[***]**

Institute of Physics, Vietnam Academy of Science and Technology
10 Dao Tan, Ba Dinh, Hanoi, Vietnam

Received May 11, 2015

We investigate the muon anomalous magnetic moment in the context of a supersymmetric version of the economical 3-3-1 model. We compute the 1-loop contribution of superpartner particles. We show that the contribution of superparticle loops become significant when $\tan\gamma$ is large. We investigate the cases of both small and large values of $\tan\gamma$. We find the region of the parameter space where the slepton masses of a few hundred GeV are favored by the muon $g-2$ for small $\tan\gamma$ ($\tan\gamma \approx 5$). Numerical estimation gives the mass of supersymmetric particles, the mass of gauginos $m_G \approx 700$ GeV, and the light slepton mass $m_{\tilde{L}}$ of the order of $\mathcal{O}$ (100) GeV. When $\tan\gamma$ is large ($\tan\gamma \approx 60$), the charged slepton mass $m_{\tilde{L}}$ and the gaugino mass m_G are $\mathcal{O}(1)$ TeV, while the sneutrino mass ≈ 450 GeV is in the reach of the LHC.

DOI: 10.7868/S004445101512007X

1. INTRODUCTION

The muon magnetic dipole moment (MDM), written in terms of $a_\mu = (g_\mu - 2)/2$, is one of the most highly measured quantity in particle physics. The current discrepancy between the experimental value and that predicted by the Standard Model (SM), $\Delta a_\mu = a_\mu^{(exp)} - a_\mu^{(SM)}$, is 3.6σ [1]. This discrepancy demands an explanation. Efforts along both the experimental and theoretical directions are being taken to address this issue. On the theoretical side, there are models of new physics. One of these models is the class of $\mathrm{SU}(3)_C \times \mathrm{SU}(3)_L \times \mathrm{U}(1)$ (3-3-1) models [2–14]. In this class of models, the $\mathrm{SU}(2)_L$ gauge symmetry group is extended to $\mathrm{SU}(3)_L$ and has some intriguing features, which can lead to the generation number problem, dark matter, small neutrino masses and their mixing, and some problems of the early Universe [15]. Among the 3-3-1 models, there is one version called the economical 3-3-1 model (E331). The economical 3-3-1 model [14] is a model with just two Higgs triplets. The Higgs sector in the E331 model is very simple and consists of two massive neutral Higgs scalars, one massive charged Higgs boson and eight Goldstone bosons. Because of the extension of the gauge group, the 3-3-1 models contain new particles such as new Higgs and gauge bosons as well as new fermions. Due to the interactions of the muon with some new heavy particles, the 3-3-1 models can make a new contribution to the muon MDM. The muon MDM problem is also investigated in this class of models [16–19]. However, this class of models cannot probably explain the $(g-2)_\mu$ anomaly if the $\mathrm{SU}(3)_L$ symmetry breaking scale is larger than $\mathcal{O}(1)$ TeV [20, 21].

Supersymmetry (SUSY) is one of the most promising candidates for the new physics beyond the Standard Model. In SUSY models, the Higgs sector is very constrained and the quadratic divergences cancel, which offers a solution to the naturalness problem [22]. In addition, precision measurements of the gauge coupling constants strongly suggest a SUSY grand unified theory [23].

There are works in which the muon MDM is calculated in the framework of SUSY models [24]. In the minimal supersymmetric standard model (MSSM) [25], the SUSY contribution is proportional to $\tan\beta$, which is the ratio of the vacuum expectation values of two Higgs fields and the suppression factor

$$\left(\frac{m_\mu}{M_{SUSY}}\right)^2.$$

If $\tan\beta$ is large, then a_μ^{SUSY} can be as large as Δa_μ [1] or if low-energy SUSY exits, the SUSY contribution to

[*]E-mail: dtbinh@iop.vast.ac.vn
[**]E-mail: dthuong@iop.vast.ac.vn
[***]E-mail: hnlong@iop.vast.ac.vn

the muon $g-2$ can be large enough to address the muon MDM anomaly, providing the masses of supersymmetry particles of the order $\mathcal{O}$ (100) GeV or $\mathcal{O}$ (1) TeV, which are within reach of the LHC. Thus, the muon MDM can possibly originate from SUSY contributions.

It is natural to investigate the muon MDM in the SUSY version of the 3-3-1 models. In this paper we investigate the muon MDM in the framework of the supersymmetric version of the economical 331 model (SUSYE331). The SUSY version of the economical 3-3-1 model (SUSYE331) was proposed in [26]. In the SUSYE331 model, the region of the parameter space can be expanded compared to that of the MSSM. It was shown in [27, 28] that the interesting region of the parameter space to study the lepton flavor violating decay process [29] can be expanded to the limit of small values of $\tan\gamma$, and the slepton mass of at least one generation can be taken in the $\mathcal{O}(100)$ GeV energy range.

We first derive analytic expressions for all one-loop contributions coming from the SUSYE331 and show that the contribution of the SUSYE331 model to the muon MDM is proportional to the values of $\tan\gamma$ and inversely proportional to the values of the slepton masses. We demonstrate the magnitude of the contribution to the muon MDM for each choice of the value of the $\tan\gamma$. Because of the appearance of new particles in the SUSYE331, we expect finding an interesting region of the SUSY parameter space in the limit of small $\tan\gamma$. We are particularly interested in exploring some numerical results of the SUSYE331 contribution to the muon MDM in the limits where the SUSYE331 slepton and gaugino masses are of the order of TeV, at small values of $\tan\gamma$.

This paper is organized as follows. In Sec. 2, we briefly review the SUSYE331 model. In Sec. 3, we discuss the neutralino and chargino sectors of the model. Sections 4 and 5 are devoted for diagonalizing the mass matrix of the smuon and sneutrino and the muon–chargino–sneutrino interaction. In Sec. 6, we calculate the muon MDM in a weak eigenstate. Section 7 is devoted to numerical calculations and bounds on masses. We summarize our results in Sec. 8.

2. REVIEW OF THE MODEL

In this section, we first recapitulate the basic elements of the supersymmetric economical 3-3-1 model [26]. The superfield content in this paper is defined as

$$\widehat{F} = (\widetilde{F}, F), \quad \widehat{S} = (S, \widetilde{S}), \quad \widehat{V} = (\lambda, V), \qquad (1)$$

where the components F, S, and V stand for the fermion, scalar, and vector fields, while their respective superpartners are denoted by $\widetilde{F}$, $\widetilde{S}$, and λ.

The superfield content of the model with an ananomaly-free fermionic content transforms under the 3-3-1 gauge group as

$$\widehat{L}_{aL} = \left(\widehat{\nu}_a, \widehat{l}_a, \widehat{\nu}_a^c\right)_L^T \sim (1, 3, -1/3), \quad \widehat{l}_{aL}^c \sim (1, 1, 1),$$

$$\widehat{Q}_{1L} = \left(\widehat{u}_1,\ \widehat{d}_1,\ \widehat{u}'\right)_L^T \sim (3, 3, 1/3),$$

$$\widehat{u}_{1L}^c,\ \widehat{u}_L'^c \sim (3^*, 1, -2/3), \quad \widehat{d}_{1L}^c \sim (3^*, 1, 1/3),$$

$$\widehat{Q}_{\alpha L} = \left(\widehat{d}_\alpha, -\widehat{u}_\alpha, \widehat{d}'_\alpha\right)_L^T \sim (3, 3^*, 0), \quad \alpha = 2, 3,$$

$$\widehat{u}_{\alpha L}^c \sim (3^*, 1, -2/3), \quad \widehat{d}_{\alpha L}^c,\ \widehat{d}_{\alpha L}'^c \sim (3^*, 1, 1/3),$$

where the values in the parentheses denote quantum numbers based on the $(\mathrm{SU}(3)_C, \mathrm{SU}(3)_L, \mathrm{U}(1)_X)$ symmetry, $\widehat{\nu}_L^c = (\widehat{\nu}_R)^c$, and $a = 1, 2, 3$ is the generation index. The primes on usual quark types (u' and d' with the electric charge $q_{u'} = 2/3$ and d' with $q_{d'} = -1/3$) indicate that those quarks are exotic ones.

The two superfields $\widehat{\chi}$ and $\widehat{\rho}$ are introduced to span the scalar sector of the economical 3-3-1 model [14]:

$$\widehat{\chi} = \left(\widehat{\chi}_1^0, \widehat{\chi}^-, \widehat{\chi}_2^0\right)^T \sim (1, 3, -1/3),$$

$$\widehat{\rho} = \left(\widehat{\rho}_1^+, \widehat{\rho}^0, \widehat{\rho}_2^+\right)^T \sim (1, 3, 2/3).$$

To cancel the chiral anomalies of the higgsino sector, two extra superfields $\widehat{\chi}'$ and $\widehat{\rho}'$ must be added:

$$\widehat{\chi}' = \left(\widehat{\chi}_1'^0, \widehat{\chi}'^+, \widehat{\chi}_2'^0\right)^T \sim (1, 3^*, 1/3),$$

$$\widehat{\rho}' = \left(\widehat{\rho}_1'^-, \widehat{\rho}'^0, \widehat{\rho}_2'^-\right)^T \sim (1, 3^*, -2/3).$$

In this model, the $\mathrm{SU}(3)_L \otimes \mathrm{U}(1)_X$ gauge group is broken in two steps:

$$\mathrm{SU}(3)_L \otimes \mathrm{U}(1)_X \xrightarrow{w,w'} \mathrm{SU}(2)_L \otimes \mathrm{U}(1)_Y \xrightarrow{v,v',u,u'} \mathrm{U}(1)_Q, \qquad (2)$$

where the VEVs are defined by

$$\begin{aligned} &\sqrt{2}\langle\chi\rangle^T = (u, 0, w), \quad \sqrt{2}\langle\chi'\rangle^T = (u', 0, w'), \\ &\sqrt{2}\langle\rho\rangle^T = (0, v, 0), \quad \sqrt{2}\langle\rho'\rangle^T = (0, v', 0). \end{aligned} \qquad (3)$$

The VEVs w and w' are responsible for the first step of the symmetry breaking, while u, u' and v, v' are for the second step. Therefore, they have to satisfy the constraints

$$u,\ u',\ v,\ v' \ll w,\ w'. \tag{4}$$

The vector superfields $\widehat{V}_c$, $\widehat{V}$, and $\widehat{V}'$ containing the usual gauge bosons are respectively associated with the $\mathrm{SU}(3)_C$, $\mathrm{SU}(3)_L$, and $\mathrm{U}(1)_X$ group factors. The color and flavor vector superfields have expansions in the Gell-Mann matrix basis $T^a = \lambda^a/2$ $(a = 1, 2, \ldots, 8)$ as

$$\widehat{V}_c = \frac{1}{2}\lambda^a \widehat{V}_{ca}, \quad \widehat{\overline{V}}_c = -\frac{1}{2}\lambda^{a*}\widehat{V}_{ca};$$
$$\widehat{V} = \frac{1}{2}\lambda^a \widehat{V}_a, \quad \widehat{\overline{V}} = -\frac{1}{2}\lambda^{a*}\widehat{V}_a,$$

where the overbar indicates complex conjugation. The vector superfields associated with $\mathrm{U}(1)_X$ are normalized as

$$X\hat{V}' = (XT^9)\hat{B}, \quad T^9 \equiv \frac{1}{\sqrt{6}}\mathrm{diag}(1,1,1).$$

The gluons are denoted by g^a and their gluino partners by λ_c^a, with $a = 1, \ldots, 8$. In the electroweak sector, V^a and B stand for the respective $\mathrm{SU}(3)_L$ and $\mathrm{U}(1)_X$ gauge bosons with their gaugino partners λ_V^a and λ_B.

With the above superfields, the full Lagrangian is defined by $\mathcal{L}_{SUSY} + \mathcal{L}_{soft}$ where the first term is the supersymmetric part, whereas the last term breaks the supersymmetry explicitly. The interested reader can find more details about the Lagrangian in [26]. In what follows, we are only interested in terms relevant to our calculations.

3. THE NEUTRALINOS AND CHARGINO SECTORS

In the SUSYE331 model, the neutralinos are mixed by an 11×11 matrix and the charginos are mixed by a 5×5 matrix. It is difficult to find the exact mass eigenstates of these mass matrices. Hence, we have to find the approximation method.

3.1. The neutralino sector

The neutralino mass terms are given in [30] as follows:

$$\mathcal{L} = \left(\widetilde{\psi^o}\right)^\dagger M_{\widetilde{N}} \widetilde{\psi^o}, \tag{5}$$

with

$$\widetilde{\psi}^o = \Big(\widetilde{\chi_1^o}, \widetilde{\chi_1^{o\prime}}, \widetilde{\chi_2^o}, \widetilde{\chi_2^{o\prime}}, \widetilde{\rho_1^o}, \widetilde{\rho_1^{o\prime}}, \lambda_B, \lambda_3, \lambda_8, \lambda_X = \frac{\lambda_4 + i\lambda_5}{2}, \lambda_{X^*} = \frac{\lambda_4 - i\lambda_5}{2}\Big),$$

and the mass matrix $M_{\widetilde{N}}$ has the form

$$M_{\widetilde{N}} = \begin{pmatrix}
0 & -\mu_\chi & 0 & 0 & 0 & 0 & -\frac{g'u}{3\sqrt{6}} & \frac{gu}{2} & \frac{gu}{2\sqrt{3}} & \frac{gw}{\sqrt{2}} & 0 \\
-\mu_\chi & 0 & 0 & 0 & 0 & 0 & \frac{g'u'}{3\sqrt{6}} & \frac{gu'}{2} & \frac{gu'}{2\sqrt{3}} & \frac{gw'}{\sqrt{2}} & 0 \\
0 & 0 & 0 & & -\mu_\chi & 0 & -\frac{g'w}{3\sqrt{6}} & 0 & -\frac{gw}{\sqrt{3}} & 0 & \frac{gu}{\sqrt{2}} \\
0 & 0 & -\mu_\chi & 0 & 0 & 0 & \frac{g'w'}{3\sqrt{6}} & 0 & -\frac{gw'}{\sqrt{3}} & 0 & \frac{gu'}{\sqrt{2}} \\
0 & 0 & 0 & 0 & 0 & -\mu_\rho & \frac{2g'v}{3\sqrt{6}} & -\frac{gv}{2} & \frac{gv}{2\sqrt{3}} & 0 & 0 \\
0 & 0 & 0 & 0 & -\mu_\rho & 0 & -\frac{2g'v'}{3\sqrt{6}} & -\frac{gv'}{2} & \frac{gv'}{2\sqrt{3}} & 0 & 0 \\
-\frac{g'u}{3\sqrt{6}} & \frac{g'u'}{3\sqrt{6}} & -\frac{g'w}{3\sqrt{6}} & \frac{g'w'}{3\sqrt{6}} & \frac{2g'v}{3\sqrt{6}} & -\frac{2g'v'}{3\sqrt{6}} & m_B & 0 & 0 & 0 & 0 \\
\frac{gu}{2} & \frac{gu'}{2} & 0 & 0 & -\frac{gv}{2} & -\frac{gv'}{2} & 0 & m_{\lambda_3} & 0 & 0 & 0 \\
\frac{gu}{2\sqrt{3}} & \frac{gu'}{2\sqrt{3}} & -\frac{gw}{\sqrt{3}} & -\frac{gw'}{\sqrt{3}} & \frac{gv}{2\sqrt{3}} & \frac{gv'}{2\sqrt{3}} & 0 & 0 & m_{\lambda_8} & 0 & 0 \\
\frac{gw}{2} & \frac{gw'}{2} & 0 & 0 & 0 & 0 & 0 & 0 & 0 & m_{\lambda_{45}} & 0 \\
0 & 0 & \frac{gu}{2} & \frac{gu'}{2} & 0 & 0 & 0 & 0 & 0 & 0 & m_{\lambda_{45}}
\end{pmatrix}, \tag{6}$$

where $m_{\lambda_4} = m_{\lambda_5} \equiv m_{\lambda_{45}}$.

In general, we can find a new basis in which the mass matrix $M_{\widetilde{N}}$ has the diagonal form by finding a unitary matrix N such that

$$N^* M_{\widetilde{N}} N^\dagger = \mathrm{diag}(m^2_{\widetilde{\chi}_1}, m^2_{\widetilde{\chi}_2}, m^2_{\widetilde{\chi}_3}, m^2_{\widetilde{\chi}_4}, m^2_{\widetilde{\chi}_5}, m^2_{\widetilde{\chi}_6}, m^2_{\widetilde{\chi}_7}, m^2_{\widetilde{\chi}_8}, m^2_{\widetilde{\chi}_9}, m^2_{\widetilde{\chi}_{10}}, m^2_{\widetilde{\chi}_{11}}).$$

As in [30], we assume that

$$v, v', u, u', w, w' \ll |\mu_\rho - m_B|, |\mu_\rho - m_{\lambda_3}|, |\mu_\rho - m_{\lambda_8}|, |\mu_\rho - m_{\lambda_{45}}| \quad (7)$$

and

$$v, v', u, u', w, w' \ll |\mu_\chi - m_B|, |\mu_\chi - m_{\lambda_3}|, |\mu_\chi - m_{\lambda_8}|, |\mu_\chi - m_{\lambda_{45}}|. \quad (8)$$

In these limits, we obtain the neutralino mass eigenstates by using the perturbation theory. In the first order of the perturbation, we obtain the mixing matrix

$$N = \begin{pmatrix}
0 & 0 & 0 & 0 & 0 & 0 & 1 & 0 & 0 & 0 & 0 \\
0 & 0 & 0 & 0 & 0 & 0 & 0 & 1 & 0 & 0 & 0 \\
0 & 0 & 0 & 0 & 0 & 0 & 0 & 0 & 1 & 0 & 0 \\
0 & 0 & 0 & 0 & 0 & 0 & 0 & 0 & 0 & 1 & 0 \\
0 & 0 & 0 & 0 & 0 & 0 & 0 & 0 & 0 & 0 & 1 \\
0 & 0 & 0 & 0 & \frac{1}{\sqrt{2}} & \frac{1}{\sqrt{2}} & 0 & 0 & 0 & 0 & 0 \\
0 & 0 & 0 & 0 & \frac{1}{\sqrt{2}} & -\frac{1}{\sqrt{2}} & 0 & 0 & 0 & 0 & 0 \\
\frac{1}{\sqrt{2}} & \frac{1}{\sqrt{2}} & 0 & 0 & 0 & 0 & 0 & 0 & 0 & 0 & 0 \\
\frac{1}{\sqrt{2}} & -\frac{1}{\sqrt{2}} & 0 & 0 & 0 & 0 & 0 & 0 & 0 & 0 & 0 \\
0 & 0 & \frac{1}{\sqrt{2}} & \frac{1}{\sqrt{2}} & 0 & 0 & 0 & 0 & 0 & 0 & 0 \\
0 & 0 & \frac{1}{\sqrt{2}} & -\frac{1}{\sqrt{2}} & 0 & 0 & 0 & 0 & 0 & 0 & 0
\end{pmatrix}.$$

Its mass eigenvalues as studied in [30].

3.2. Chargino sector

In the SUSYE331 model, there are four charged gauginos and six charged Higgsinos. In the basis

$$\psi^+ = (\lambda_{\widetilde{\mathcal{W}}^+}, \lambda_{\widetilde{\mathcal{Y}}^+}, \widetilde{\rho_1}^+, \widetilde{\rho_2}^+, \widetilde{\chi}'^+),$$

$$\psi^- = (\lambda_{\widetilde{\mathcal{W}}^-}, \lambda_{\widetilde{\mathcal{Y}}^-}, \widetilde{\rho_1}'^-, \widetilde{\rho_2}'^-, \widetilde{\chi}^-),$$

the Lagrangian describes the chargino mass terms as

$$\mathcal{L}_{chargino\ mass} = \left(\widetilde{\psi}^\pm\right)^+ M_{\widetilde{\psi}} \widetilde{\psi}^\pm + \mathrm{H.c.},$$

where

$$M_{\widetilde{\psi}} = \begin{pmatrix} 0 & \mathcal{M} \\ \mathcal{M}^T & 0 \end{pmatrix},$$

with the 5×5 matrix

$$\mathcal{M} = \begin{pmatrix}
m_{\lambda_W} & 0 & \frac{gv'}{\sqrt{2}} & 0 & \frac{gu}{\sqrt{2}} \\
0 & m_{\lambda_Y} & 0 & \frac{gv'}{\sqrt{2}} & \frac{gw}{\sqrt{2}} \\
\frac{gv}{\sqrt{2}} & 0 & \mu_\rho & 0 & 0 \\
0 & \frac{gv}{\sqrt{2}} & 0 & \mu_\rho & 0 \\
\frac{gu'}{\sqrt{2}} & \frac{gw'}{\sqrt{2}} & 0 & 0 & \mu_\chi
\end{pmatrix}.$$

To diagonalize the chargino mass matrix, we have to find two unitary 5×5 matrices U and V such that

$$U^* \mathcal{M} V^\dagger = \begin{pmatrix}
m_{\lambda_W} & 0 & 0 & 0 & 0 \\
0 & m_2 & 0 & 0 & 0 \\
0 & 0 & \mu_\rho & 0 & 0 \\
0 & 0 & 0 & m_3 & 0 \\
0 & 0 & 0 & 0 & \mu_\rho
\end{pmatrix} \equiv \mathrm{diag}(m^\pm_{\chi_1}, m^\pm_{\chi_2}, m^\pm_{\chi_3}, m^\pm_{\chi_4}, m^\pm_{\chi_5}),$$

where

$$m_2 = \frac{1}{4}\left[2(\mu_\chi^2 + m_{\lambda_Y}^2) + g^2(w^2 + w'^2) - \sqrt{(2(\mu_\chi + m_{\lambda_Y})^2 + g^2(w - w')^2)\,(2(\mu_\chi - m_{\lambda_Y})^2 + g^2(w + w')^2)}\right],$$

$$m_3 = \frac{1}{4}\left[2(\mu_\chi^2 + m_{\lambda_Y}^2) + g^2(w^2 + w'^2) + \sqrt{(2(\mu_\chi + m_{\lambda_Y})^2 + g^2(w - w')^2)\,(2(\mu_\chi - m_{\lambda_Y})^2 + g^2(w + w')^2)}\right].$$

To find the matrices U and V we have to diagonalize the matrix $M^\dagger M$ by finding the matrix C such that $C^\dagger M^\dagger M C \equiv M_D^2$, where M_D has a diagonal form. The matrices U and V are represented as

$$V^\dagger = C, \quad U^\star = M_D^{-1} C^\dagger M^\dagger.$$

In the leading order in $m_{\lambda_W}, m_{\lambda_Y}, \mu_\rho, \mu_\chi, w, w' \gg u, u'v, v'$, the matrix C has the form

$$C = \begin{pmatrix} 1 & 0 & 0 & 0 & 0 \\ 0 & \dfrac{A}{\sqrt{1+A^2}} & 0 & \dfrac{B}{\sqrt{1+B^2}} & 0 \\ 0 & 0 & 1 & 0 & 0 \\ 0 & 0 & 0 & 0 & 1 \\ 0 & \dfrac{1}{\sqrt{1+A^2}} & 0 & \dfrac{1}{\sqrt{1+B^2}} & 0 \end{pmatrix},$$

and the matrix U^* is

$$U^* = \begin{pmatrix} 1 & 0 & \dfrac{gv}{\sqrt{2}m_{\lambda_W}} & 0 & \dfrac{gu'}{\sqrt{2}m_{\lambda_W}} \\ \dfrac{gu}{\sqrt{2(1+A^2)^2}m_2} & \dfrac{2Am_{\lambda_Y} + \sqrt{2}gw}{2\sqrt{1+A^2}\,m_2} & 0 & \dfrac{gvA}{\sqrt{2(1+A^2)}m_2} & \dfrac{2\mu_\chi + \sqrt{2}Agw'}{2\sqrt{1+A^2}\,m_2} \\ \dfrac{gv'}{\sqrt{2}\mu_\rho} & 0 & 1 & 0 & 0 \\ \dfrac{gu}{\sqrt{2(1+B^2)}m_3} & \dfrac{2Bm_{\lambda_Y} + \sqrt{2}gw}{2\sqrt{1+B^2}\,m_3} & 0 & \dfrac{Bgv}{\sqrt{2(1+B^2)}m_3} & \dfrac{2\mu_\chi + \sqrt{2}gw'B}{\sqrt{2(1+B^2)}m_3} \\ 0 & \dfrac{gv'}{\sqrt{2}\mu_\rho} & 0 & 1 & 0 \end{pmatrix},$$

where

$$A = \frac{1}{2\sqrt{2}(m_{\lambda_Y} w + \mu_\chi w')}\left(2(\mu_\chi^2 - m_{\lambda_Y}^2) + g^2(w^2 - w'^2) + \right.$$
$$\left. + \sqrt{-4(-2\mu_\chi m_{\lambda_Y} + g^2 w w')^2 + (2(\mu_\chi^2 + m_{\lambda_Y}^2) + g^2(w^2 + w'^2))^2}\right),$$
$$B = \frac{1}{2\sqrt{2}(m_{\lambda_Y} w + \mu_\chi w')}\left(-2(\mu_\chi^2 - m_{\lambda_Y}^2) - g^2(w^2 - w'^2) + \right.$$
$$\left. + \sqrt{-4(-2\mu_\chi m_{\lambda_Y} + g^2 w w')^2 + (2(\mu_\chi^2 + m_{\lambda_Y}^2) + g^2(w^2 + w'^2))^2}\right).$$

4. SMUON AND SNEUTRINO MASSES

The superpotential of the model under consideration relevant to the contribution to $(g-2)_\mu$ is given by

$$W' = \mu_{0a}\hat{L}_{aL}\hat{\chi}' + \mu_\chi \hat{\chi}\hat{\chi}' + \mu_\rho \hat{\rho}\hat{\rho}' + $$
$$+ \gamma_{ab}\hat{L}_{aL}\hat{\rho}'\hat{l}^c_{bL} + \lambda a \epsilon \hat{L}_{aL}\hat{\chi}\hat{\rho} + \lambda'_{ab}\epsilon\hat{L}_{aL}\hat{L}_{bL}\hat{\rho},$$

where μ_{0a}, μ_ρ, and μ_χ have the dimension mass, the other coefficients in W' are dimensionless, and $\lambda'_{ab} = -\lambda'_{ba}$.

The relevant softly breaking terms are obtained as

$$-\mathcal{L}_{SMT} = M_{ab}^2 \widetilde{L}^\dagger_{aL}\widetilde{L}_{bL} + m_{ab}^2 \widetilde{l}^{c*}_{aL}\widetilde{l}^c_{bL} +$$
$$+ \Big\{ M'^2_a \chi^\dagger \widetilde{L}_{aL} + \eta_{ab}\widetilde{L}_{aL}\rho'\widetilde{l}^c_{Lb} + \upsilon_a \epsilon \widetilde{L}_{aL}\chi\rho +$$
$$+ \varepsilon_{ab}\epsilon\widetilde{L}_{aL}\widetilde{L}_{bL}\rho + \omega_{a\alpha j}\widetilde{L}_{aL}\widetilde{Q}_{\alpha L}\widetilde{d}^c_{jL} +$$
$$+ \omega'_{a\alpha\beta}\widetilde{L}_{aL}\widetilde{Q}_{\alpha L}\widetilde{d}'^c_{\beta L} + \text{H.c.}\Big\}, \quad (9)$$

where $\varepsilon_{ab} = -\varepsilon_{ba}$. This Lagrangian is also responsible for sfermion masses. The sfermion masses are obtained by combining the soft terms, D-terms, and F-terms. The interested reader can find the details in [31]. In general, there is flavor mixing in the slepton mass matrix. However, large flavor mixing in the slepton sector can create a mismatch for the lepton flavor decay processes of the muon and the tauon [27, 28]. In this work, we assume that the flavor mixing matrix elements are not too large. We can then ignore all the flavor mixing terms. The mass matrix for the smuon can be written as

$$M_{smuon} = \begin{pmatrix} m^2_{\tilde{\mu}L} & m^2_{\tilde{\mu}LR} \\ m^2_{\tilde{\mu}LR} & m^2_{\tilde{\mu}R} \end{pmatrix}, \tag{10}$$

where

$$m^2_{\tilde{\mu}L} = M^2_{22} + \frac{1}{4}\mu^2_{02} + \frac{g^2}{2}\left(-H_3 + \frac{1}{\sqrt{3}}H_8 - \frac{2t^2}{3}H_1\right) + \\ + \frac{v'^2}{18}\gamma^2_{22} + \frac{1}{18}\lambda^2_2(u^2+w^2), \tag{11}$$

$$m^2_{\tilde{\mu}R} = \left(m^2_{22} + \frac{v'^2}{18}\gamma^2_{22} + g^2t^2H_1\right), \\ m^2_{\tilde{\mu}LR} = \frac{1}{\sqrt{2}}\left(\eta_{22}v' + \frac{1}{6}\mu_\rho\gamma_2 v\right), \tag{12}$$

with

$$H_3 = -\frac{1}{4}\left(u^2\frac{\cos 2\beta}{s^2_\beta} + v^2\frac{\cos 2\gamma}{c^2_\gamma}\right), \tag{13}$$

$$H_8 = \frac{1}{4\sqrt{3}}\left[v^2\frac{\cos 2\gamma}{c^2_\gamma} - (u^2 - 2w^2)\frac{\cos 2\beta}{s^2_\beta}\right], \tag{14}$$

$$H_4 = -\frac{1}{2}uw\frac{\cos 2\beta}{s^2_\beta}, \tag{15}$$

$$H_1 = \frac{1}{6}\left[(u^2+w^2)\frac{\cos 2\beta}{s^2_\beta} + 2v^2\frac{\cos 2\gamma}{c^2_\gamma}\right], \tag{16}$$

and

$$\tan\beta = \frac{u}{u'} = \frac{w}{w'}, \quad \tan\gamma = \frac{v'}{v}, \\ s_\beta = \sin\beta, \quad c_\beta = \cos\beta.$$

Diagonalizing the mass matrix in Eq. (10), we can obtain the mass eigenvalues

$$m^2_{\tilde{\mu}_L} = \frac{1}{2}\left(m^2_{\tilde{\mu}L} + m^2_{\tilde{\mu}R} - \Delta\right), \tag{17}$$

$$m^2_{\tilde{\mu}_R} = \frac{1}{2}\left(m^2_{\tilde{\mu}L} + m^2_{\tilde{\mu}R} + \Delta\right), \tag{18}$$

where

$$\Delta = \sqrt{\left(m^2_{\tilde{\mu}L} - m^2_{\tilde{\mu}R}\right)^2 + 4m^4_{\tilde{\mu}LR}}.$$

The mass eigenstates are

$$\begin{pmatrix} \tilde{\mu}_L \\ \tilde{\mu}_R \end{pmatrix} = \begin{pmatrix} s_{\theta_{\tilde{\mu}}} & -c_{\theta_{\tilde{\mu}}} \\ c_{\theta_{\tilde{\mu}}} & s_{\theta_{\tilde{\mu}}} \end{pmatrix} \begin{pmatrix} l_{\tilde{\mu}_R} \\ l_{\tilde{\mu}_L} \end{pmatrix} \equiv \\ \equiv U^{-1}_{\tilde{\mu}} \begin{pmatrix} l_{\tilde{\mu}_R} \\ l_{\tilde{\mu}_L} \end{pmatrix}, \tag{19}$$

$$\tilde{\mu}_L = c_{\theta_{\tilde{\mu}}} l_{\tilde{\mu}_R} - s_{\theta_{\tilde{\mu}}} l_{\tilde{\mu}_L}, \\ \tilde{\mu}_R = s_{\theta_{\tilde{\mu}}} l_{\tilde{\mu}_R} + c_{\theta_{\tilde{\mu}}} l_{\tilde{\mu}_L},$$

where $s_{\theta_{\tilde{\mu}}} = \sin\theta_{\tilde{\mu}}$, $c_{\theta_{\tilde{\mu}}} = \cos\theta_{\tilde{\mu}}$, and $\theta_{\tilde{\mu}}$ is defined through $\tan 2\theta_{\tilde{\mu}}$ as follows:

$$\tan 2\theta_{\tilde{\mu}} = t_{2\theta_{\tilde{\mu}}} = \frac{2m^2_{\tilde{\mu}LR}}{m^2_{\tilde{\mu}L} - m^2_{\tilde{\mu}R}}.$$

Next, we study the muon sneutrino mass. If we ignore the mixing among sneutrinos of the first two generations, the sneutrino mass $m_{\tilde{\nu}_\mu}$ takes the form

$$m^2_{\tilde{\nu}_{\mu L}} = M^2_{22} + \frac{1}{4}\mu^2_{02} + \frac{g^2}{2}\left(H_3 + \frac{1}{\sqrt{3}}H_8 - \frac{2t^2}{3}H_1\right) + \\ + \frac{1}{18}v^2(\lambda^2_2 + 4\lambda'^2_{c2}) + \frac{1}{18}\lambda^2_2 w^2, \tag{20}$$

$$m^2_{\tilde{\nu}_{\mu R}} = M^2_{22} + \frac{1}{4}\mu^2_{02} - g^2\left(\frac{1}{\sqrt{3}}H_8 + \frac{t^2}{3}H_1\right) + \\ + \frac{1}{18}v^2(\lambda^2_2 + 4\lambda'^2_{c2}) + \frac{1}{18}\lambda^2_2 u^2. \tag{21}$$

5. MUON–NEUTRALINO–SMUON AND MUON–CHARGINO–SNEUTRINO VERTICES

The interaction terms contain the lepton–neutralino–slepton and lepton–chargino–sneutrino vertices:

$$L_{l\tilde{l}\tilde{V}} = -\frac{ig}{\sqrt{2}}\left(\overline{L}\lambda^a\widetilde{L}\overline{\lambda}^a_V - \overline{\widetilde{L}}\lambda^a L\lambda^a_V\right) - ig'\sqrt{\frac{1}{3}} \times \\ \times\left[-\frac{1}{3}\left(\overline{L}\widetilde{L}\overline{\lambda}_B - \overline{\widetilde{L}}L\lambda_B\right) + \left(\overline{l}^c\widetilde{l}^c\overline{\lambda}_B - \overline{\widetilde{l}}^c l^c\lambda_B\right)\right], \tag{22}$$

$$L_{l\tilde{l}\tilde{H}} = -\frac{\lambda_{1ab}}{3}\left(L_a\widetilde{\rho}'\widetilde{l^c_b} + \widetilde{L_a}\widetilde{\rho}' l^c_b\right) - \\ - \frac{\lambda_{3ab}}{3}\left(L_a\widetilde{\rho}\widetilde{L_b} + \widetilde{L_a}\widetilde{\rho}L_b\right) + \text{H.c.} \tag{23}$$

We recall that the lepton number is conserved in the lepton sector at the tree level and λ_{3ab} are antisymmetric with the vanishing couplings λ_{1ab} and λ_{3ab} if a equals b. We use the notations $Y_\mu = \lambda_{122}/3$ as given in [28]. Expanding Eqs. (22) and (23), we rewrite only the muon–neutralino–smuon and muon–chargino–sneutrino interaction terms. All the relevant terms are given by

$$L_{\mu\tilde{\mu}\tilde{V}} = \overline{\mu}_L \left(\frac{ig'}{3\sqrt{3}}\overline{\lambda}_B + \frac{ig}{\sqrt{2}} \left(\overline{\lambda_A^3} - \frac{1}{\sqrt{3}}\overline{\lambda_A^8} \right) \right) \widetilde{\mu}_L - \\ - \mu_L \left(\frac{ig'}{3\sqrt{3}}\lambda_B + \frac{ig}{\sqrt{2}} \left(\lambda_A^3 - \frac{1}{\sqrt{3}}\lambda_A^8 \right) \right) \widetilde{\mu}_L^* - i\frac{g'}{\sqrt{3}} \times \\ \times \left(\bar{\mu}^c \widetilde{\mu^c} \lambda_B^- - \overline{\widetilde{\mu^c}} \mu^c \lambda_B \right) - ig \left(\overline{\mu}_L \overline{\widetilde{W}^+} \widetilde{\nu}_{\mu L} - \mu_L \widetilde{W}^+ \widetilde{\nu}_{\mu L}^* \right) + \\ + ig \left(\overline{\mu}_L \overline{\widetilde{Y}^+} \widetilde{\nu}_{\mu L} - \mu_L \widetilde{Y}^+ \widetilde{\nu}_{\mu L}^* \right), \quad (24)$$

$$L_{\mu\tilde{\mu}\tilde{H}} = -Y_\mu \{ \mu_L \widetilde{\mu}_L^c \widetilde{\rho}'^o + \widetilde{\mu}_L \widetilde{\rho}'^o \mu_L^c + \\ + \widetilde{\nu}_{\mu L} \widetilde{\rho}_1'^- \mu_L^c + \widetilde{\nu}_{\mu L}^c \widetilde{\rho}_2'^- \mu_L^c \} + \text{H.c.} \quad (25)$$

Equations (24) and (25) can be written in the physical states as follows:

$$L_{\mu\tilde{\mu}\chi_i} = \sum_{iA} \overline{\mu} (P_R N^R_{\chi_i \tilde{\mu}_A} + P_L N^L_{\chi_i \tilde{\mu}_A}) \widetilde{\mu}_A \overline{\chi}_i + \\ + \sum_{jB} \overline{\mu} (P_R C^R_{\chi_j \tilde{\nu}_B} + P_L C^L_{\chi_j \tilde{\nu}_B}) \overline{\chi_j^+} \widetilde{\nu}_A + \text{H.c.}, \quad (26)$$

where

$$N^L_{\chi_i \tilde{\mu}_A} = \left(\frac{ig'}{3\sqrt{3}} N^*_{7i} + \frac{ig}{\sqrt{2}} N^*_{8i} - \frac{ig}{\sqrt{6}} N^*_{9i} \right) \times \\ \times (U_{\tilde{\mu}})_{LA} - Y_\mu N^*_{6i} (U_{\tilde{\mu}})_{RA},$$

$$N^R_{\chi_i \tilde{\mu}_A} = -\frac{ig'}{\sqrt{3}} N^*_{7i} (U_{\tilde{\mu}})_{RA} - Y_\mu N^*_{6i} (U_{\tilde{\mu}})_{LA},$$

$$C^L_{\chi_j \tilde{\nu}_B} = -ig \left(V_{1j} (U_\nu)_{LB} + V_{2j} (U_\nu)_{RB} \right),$$

$$C^R_{\chi_j \tilde{\nu}_B} = -Y_\mu (U_{3j} (U_\nu)_{LA} + U_{4j} (U_\nu)_{RA}).$$

6. SUSY CONTRIBUTION TO THE MUON MDM

The amplitude for the photon–muon–muon coupling in the limit of the zero photon momentum can be written as

$$M_{fi} = ie\overline{u} \left[\gamma^\alpha + a_\mu \frac{i\sigma^{\alpha\beta} q_\beta}{2m_\mu} \right] u A_\alpha.$$

The magnetic dipole moment a_μ can be calculated in both mass eigenstates and weak eigenstates. But in the next section, the magnetic dipole moment is evaluated in the weak eigenstates, because in this basis the dependence of a_μ on SUSY parameters is more apparent than in the mass eigenstate basis.

The SM prediction for the muon anomalous magnetic moment was given in [32]:

$$a_\mu^{SM} = 116591803(1)(42)(26) \cdot 10^{-11}.$$

From the recent E821 experiments [33], taking correlations between systematic errors into account, we find

$$a_\mu^{E821} = 116592091(54)(33) \cdot 10^{-11} = \\ = (116592091 \pm 63.3) \cdot 10^{-11}.$$

Hence

$$\Delta a_\mu (\text{E821} - \text{SM}) = 288(63)(49) \cdot 10^{-11} = \\ = (288 \pm 80) \cdot 10^{-11}.$$

Then Δa_μ is $3.68 \cdot 10^{-9}$ and $2.08 \cdot 10^{-9}$ at the respective levels of 3.6σ and 2.0σ.

6.1. Mass eigenstate

The effect of supersymmetry on a_μ includes loops with charginos and neutralinos. The one-loop contributions to a_μ [24], including the effects of a possible complex phase, are

$$\Delta a_\mu^{\chi^0 \tilde{\mu}} = m_\mu \times \\ \times \sum_{iA} \Big\{ -m_\mu (|N^L_{\chi_i \tilde{\mu}_A}|^2 + |N^R_{\chi_i \tilde{\mu}_A}|^2) m^2_{\tilde{\mu}A} \times \\ \times J_5(m^2_{\chi_i}, m^2_{\tilde{\mu}A}, m^2_{\tilde{\mu}A}, m^2_{\tilde{\mu}A}, m^2_{\tilde{\mu}A}) + \\ + m_{\chi_i} \operatorname{Re}(N^{L*}_{\chi_i \tilde{\mu}_A} N^R_{\chi_i \tilde{\mu}_A}) \times \\ \times J_4(m^2_{\chi_i}, m^2_{\chi_i}, m^2_{\tilde{\mu}A}, m^2_{\tilde{\mu}A}) \Big\} = \\ = \frac{1}{16\pi^2} m_\mu \sum_{iA} \Bigg\{ -\frac{m_\mu}{6 m^2_{\tilde{\mu}A} (1 - x_{\chi_i A})^4} \times \\ \times (|N^L_{\chi_i \tilde{\mu}_A}|^2 + |N^R_{\chi_i \tilde{\mu}_A}|^2) \times \\ \times (1 - 6x_{\chi_i A} + 3x^2_{\chi_i A} + 2x^3_{\chi_i A} - 6x^2_{\chi_i A} \ln x_{\chi_i A}) - \\ - \frac{m_{\chi_i}}{m^2_{\tilde{\mu}A} (1 - x_{\chi_i A})^3} \operatorname{Re}(N^{L*}_{\chi_i \tilde{\mu}_A} N^R_{\chi_i \tilde{\mu}_A}) \times \\ \times (1 - x^2_{\chi_i A} + 2x_{\chi_i A} \ln x_{\chi_i A}) \Bigg\},$$

$$\Delta a_\mu^{\chi^\pm \tilde{\nu}} = m_\mu \sum_i \Big[m_\mu (|C^L_{\chi_i \tilde{\nu}}|^2 + |C^R_{\chi_i \tilde{\nu}}|^2) \times \\ \times \{ m^2_{\tilde{\nu}} J_5(m^2_{\chi_i^\pm}, m^2_{\chi_i^\pm}, m^2_{\chi_i^\pm}, m^2_{\chi_i^\pm}, m^2_{\tilde{\nu}}) + \\ + J_4(m^2_{\chi_i^\pm}, m^2_{\chi_i^\pm}, m^2_{\chi_i^\pm}, m^2_{\chi_i^\pm}),$$

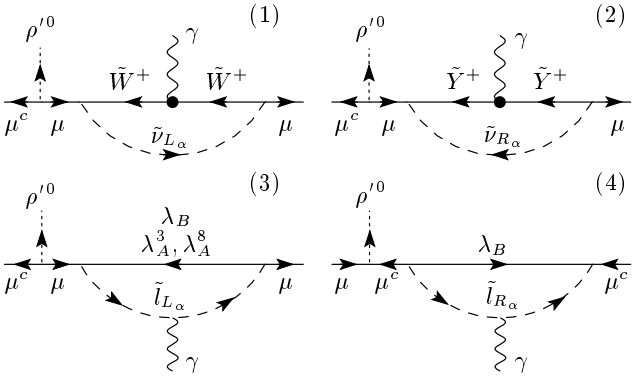

Fig. 1. Contribution to $a_{\mu L}^{(a)}$ (1–3) and $a_{\mu R}^{(a)}$ (4)

$$
\begin{aligned}
&- J_4(m^2_{\chi^\pm X}, m^2_{\chi^\pm X}, m^2_{\chi^\pm X} m^2_{\tilde\nu})\} - \\
&- 2m_X \,\mathrm{Re}(C^{L*}_{\chi_i\tilde\nu} C^R_{\chi_i\tilde\nu}) - \\
&- J_4(m^2_{\chi_i^\pm X}, m^2_{\chi_i^\pm X}, m^2_{\chi_i^\pm X}, m^2_{\tilde\nu})\Big] = \frac{1}{16\pi^2} m_\mu \times \\
&\times \sum_i \left\{ \frac{m_\mu}{3m^2_{\tilde\nu}(1-x_{\chi_i^\pm})^4} (|C^L_{\chi_i\tilde\nu}|^2 + |C^R_{\chi_i\tilde\nu}|^2) \times \right. \\
&\times \left(1 + \frac{3}{2} x_{\chi_i^\pm} - 3x^2_{\chi_i^\pm} + \frac{1}{2} x^3_{\chi_i^\pm} + 3x_{\chi_i^\pm} \ln x_{\chi_i^\pm} \right) - \\
&- \frac{3m_{\chi^\pm}}{m^2_{\tilde\nu}(1-x_{\chi_i^\pm})^3} \,\mathrm{Re}(C^{L*}_{\chi_i\tilde\nu} C^R_{\chi_i\tilde\nu}) \times \\
&\times \left. \left(1 - \frac{4}{3} x_{\chi_i^\pm} + \frac{1}{3} x^2_{\chi_i^\pm} + \frac{2}{3} \ln x_{\chi_i^\pm} \right) \right\},
\end{aligned}
\tag{27}
$$

where $x_{\chi_i^\pm} = m^2_{\chi_i^\pm}/m^2_{\tilde\nu}$, $x_{\chi_i A} = m^2_{\chi_i}/m^2_{\mu_A^-}$.

Based on the contributions of the SUSYE331 model to the muon MDM given in Eqs. (27), it is difficult to see the effects of the SUSYE331 parameter space on the muon MDM, in particular, the role of $\tan\gamma$. To assess the effects of the SUSYE331 parameter space on the muon MDM, it is convenient to use the mass insertion method to calculate the diagrams. In what follows, we consider the muon MDM based on the weak eigenstates.

6.2. Weak eigenstates

In this section, we consider the SUSY contribution to the muon MDM by using the mass insertion method to calculate the diagrams in Figs. 1–3. The contributions to a_μ can be separated into six parts:

$$
a_\mu^{SUSYE331} = a_{\mu L}^{(a)} + a_{\mu R}^{(a)} + a_{\mu L}^{(b)} + a_{\mu R}^{(b)} + a_{\mu L}^{(c)} + a_{\mu R}^{(c)},
$$

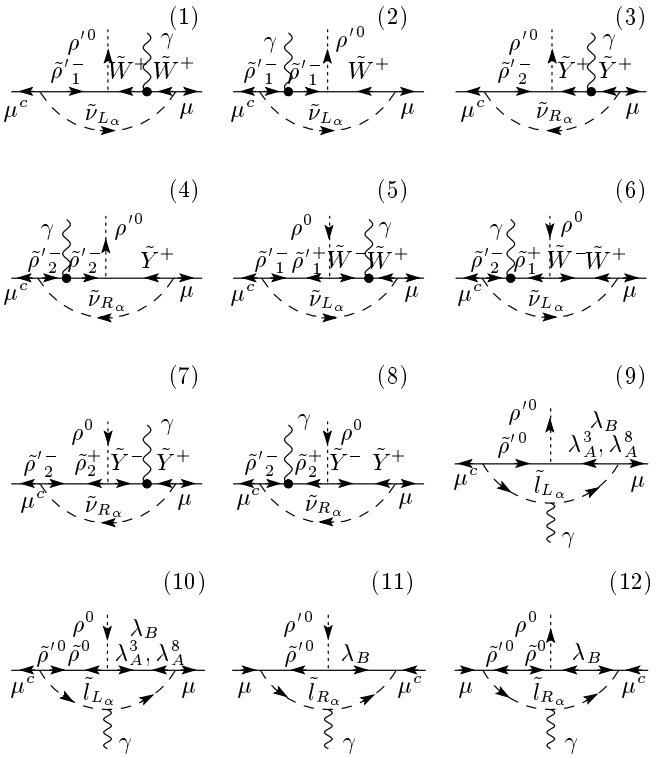

Fig. 2. Contribution to $a_{\mu L}^{(b)}$ (1–10) and $a_{\mu R}^{\mu(b)}$ (11,12)

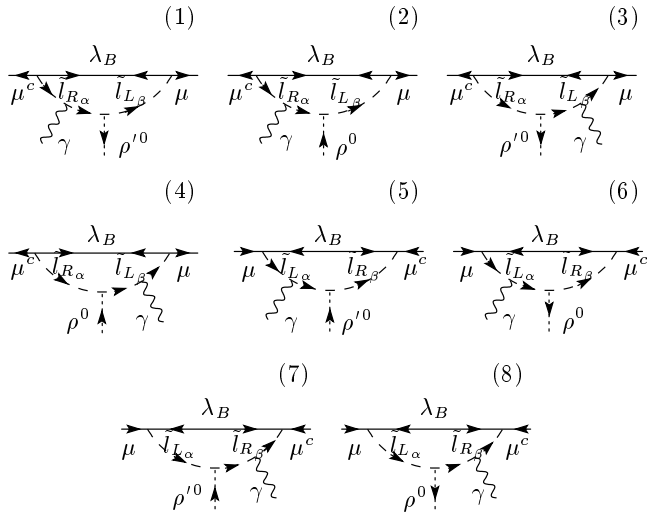

Fig. 3. Contribution to $a_{\mu L}^{(c)}$ (1–6) and $a_{\mu R}^{(c)}$ (7,8)

where the diagrams involving each part are shown in Figs. 1–3. Their contributions are

$$a_{\mu L}^{(a)} = -\frac{g^2 m_\mu^2}{8\pi^2}\left[\frac{m_{\tilde{l}_{L2}}^2 c_L^2}{3}\times\right.$$
$$\times\, J_5(m_\lambda^2, m_{\tilde{l}_{L2}}^2, m_{\tilde{l}_{L2}}^2, m_{\tilde{l}_{L2}}^2, m_{\tilde{l}_{L2}}^2) -$$
$$\left. - \frac{m_\lambda^2 c_{\nu_L}^2}{2} J_5(m_\lambda^2, m_\lambda^2, m_\lambda^2, m_\lambda^2, m_{\tilde{\nu}_{L2}}^2)\right] +$$
$$+ \frac{g^2 c_{\nu_R}^2 m_\mu^2}{8\pi^2}\,\frac{m_\lambda^2}{2} J_5(m_\lambda^2, m_\lambda^2, m_\lambda^2, m_\lambda^2, m_{\tilde{\nu}_{R2}}^2) -$$
$$-\frac{g'^2 c_L^2 m_\mu^2}{8\pi^2}\,\frac{m_{\tilde{l}_{L2}}^2}{54} J_5(m_B^2, m_{\tilde{l}_{L2}}^2, m_{\tilde{l}_{L2}}^2, m_{\tilde{l}_{L2}}^2, m_{\tilde{l}_{L2}}^2) +$$
$$+ \left(L_2 \to L_3, R_2 \to R_3, c_L^2 \to s_L^2, c_{\nu_R}^2 \to s_{\nu_R}^2\right), \quad (28)$$

$$a_{\mu R}^{(a)} = -\frac{g'^2 c_R^2 m_\mu^2}{8\pi^2}\,\frac{m_{\tilde{l}_{R2}}^2}{6}\times$$
$$\times\, J_5(m_B^2, m_{\tilde{l}_{R2}}^2, m_{\tilde{l}_{R2}}^2, m_{\tilde{l}_{R2}}^2, m_{\tilde{l}_{R2}}^2) +$$
$$+ \left(R_2 \to R_3, c_R^2 \to s_R^2\right), \quad (29)$$

$$a_{\mu L}^{(b)} = \frac{g^2 c_{\nu_L}^2 m_\mu^2}{8\pi^2} m_{\tilde{\nu}_{L2}}^4 I_5(m_\lambda^2, \mu_\rho^2, m_{\tilde{\nu}_{L2}}^2, m_{\tilde{\nu}_{L2}}^2, m_{\tilde{\nu}_{L2}}^2) +$$
$$+ \frac{g^2 c_{\nu_R}^2 m_\mu^2}{8\pi^2} m_{\tilde{\nu}_{R2}}^4 I_5(m_\lambda^2, \mu_\rho^2, m_{\tilde{\nu}_{R2}}^2, m_{\tilde{\nu}_{R2}}^2, m_{\tilde{\nu}_{R2}}^2) -$$
$$- \frac{g^2 c_{\nu_L}^2 m_\mu^2}{8\pi^2} m_\lambda \mu_\rho \tan\gamma \left[J_5(m_\lambda^2, m_\lambda^2, \mu_\rho^2, \mu_\rho^2, m_{\tilde{\nu}_{L2}}^2) +\right.$$
$$+ J_5(m_\lambda^2, m_\lambda^2, m_\lambda^2, \mu_\rho^2, m_{\tilde{\nu}_{L2}}^2) +$$
$$\left. + J_5(m_\lambda^2, \mu_\rho^2, \mu_\rho^2, \mu_\rho^2, m_{\tilde{\nu}_{L2}}^2)\right] -$$
$$- \frac{g^2 c_{\nu_R}^2 m_\mu^2}{8\pi^2} m_\lambda\ \mu_\rho\ \tan\gamma \left[J_5(m_\lambda^2, m_\lambda^2, \mu_\rho^2, \mu_\rho^2, m_{\tilde{\nu}_{R2}}^2) +\right.$$
$$+ J_5(m_\lambda^2, m_\lambda^2, m_\lambda^2, \mu_\rho^2, m_{\tilde{\nu}_{R2}}^2) +$$
$$\left. + J_5(m_\lambda^2, \mu_\rho^2, \mu_\rho^2, \mu_\rho^2, m_{\tilde{\nu}_{R2}}^2)\right] +$$
$$+ \frac{g^2 c_L^2 m_\mu^2}{8\pi^2} m_{\tilde{l}_{L2}}^2 \frac{2}{3}\left[J_5(m_\lambda^2, \mu_\rho^2, m_{\tilde{l}_{L2}}^2, m_{\tilde{l}_{L2}}^2, m_{\tilde{l}_{L2}}^2) -\right.$$
$$\left. - m_\lambda \mu_\rho \tan\gamma I_5(m_\lambda^2, \mu_\rho^2, m_{\tilde{l}_{L2}}^2, m_{\tilde{l}_{L2}}^2, m_{\tilde{l}_{L2}}^2)\right] -$$
$$- \frac{g'^2 c_L^2 2 m_\mu^2}{8\pi^2}\ m_{\tilde{l}_{L2}}^2 \frac{2}{27}\left[J_5(m_B^2, \mu_\rho^2, m_{\tilde{l}_{L2}}^2, m_{\tilde{l}_{L2}}^2, m_{\tilde{l}_{L2}}^2) -\right.$$
$$\left. - m_B \mu_\rho \tan\gamma I_5(m_B^2, \mu_\rho^2, m_{\tilde{l}_{L2}}^2, m_{\tilde{l}_{L2}}^2, m_{\tilde{l}_{L2}}^2)\right] +$$
$$+ \left(L_2 \to L_3, R_2 \to R_3, c_L^2 \to s_L^2,\right.$$
$$\left. c_{\nu_R}^2 \to s_{\nu_R}^2, c_{\nu_L}^2 \to s_{\nu_L}^2\right), \quad (30)$$

$$a_{\mu R}^{(b)} = -\frac{g'^2 c_R^2 m_\mu^2}{8\pi^2} m_{\tilde{l}_{R2}}^2 \frac{2}{9}\times$$
$$\times \left[-J_5(m_B^2, \mu_\rho^2, m_{\tilde{l}_{R2}}^2, m_{\tilde{l}_{R2}}^2, m_{\tilde{l}_{R2}}^2) +\right.$$
$$\left. + m_B \mu_\rho \tan\gamma I_5(m_B^2, \mu_\rho^2, m_{\tilde{l}_{R2}}^2, m_{\tilde{l}_{R2}}^2, m_{\tilde{l}_{R2}}^2)\right] +$$
$$+ \left(R_2 \to R_3, c_R^2 \to s_R^2\right), \quad (31)$$

$$a_{\mu LR}^{(c)} = \frac{g'^2 m_\mu^2}{8\pi^2}\,\frac{m_B^3}{9}\times$$
$$\times \left[\left(\frac{m_\tau}{m_\mu}\left[c_R^2 s_L c_L A_{\mu\tau}^R + s_R c_R c_L^2 A_{\mu\tau}^L\ +\right.\right.\right.$$
$$\left. + s_R c_R s_L c_L \left(A_\tau + \frac{\mu_\rho \tan\gamma}{2}\right)\right] +$$
$$\left. + c_R^2 c_L^2 \left[A_\mu + \frac{\mu_\rho \tan\gamma}{2}\right]\right) \times$$
$$\times\, I_5(m_B^2, m_B^2, m_B^2, m_{\tilde{l}_{L2}}^2, m_{\tilde{l}_{R2}}^2) +$$
$$+ \left(\frac{m_\tau}{m_\mu}\left[-c_R^2 s_L c_L A_{\mu\tau}^R + s_R c_R s_L^2 A_{\mu\tau}^L\ -\right.\right.$$
$$\left. - s_R c_R s_L c_L \left(A_\tau + \frac{\mu_\rho \tan\gamma}{2}\right)\right] +$$
$$\left. + c_R^2 s_L^2 \left[A_\mu + \frac{\mu_\rho \tan\gamma}{2}\right]\right) \times$$
$$\times\, I_5(m_B^2, m_B^2, m_B^2, m_{\tilde{l}_{L3}}^2, m_{\tilde{l}_{R2}}^2) +$$
$$+ \left(\frac{m_\tau}{m_\mu}\left[s_R^2 s_L c_L A_{\mu\tau}^R - s_R c_R c_L^2 A_{\mu\tau}^L\ -\right.\right.$$
$$\left. - s_R c_R s_L c_L \left(A_\tau + \frac{\mu_\rho \tan\gamma}{2}\right)\right] +$$
$$\left. + s_R^2 c_L^2 \left[A_\mu + \frac{\mu_\rho \tan\gamma}{2}\right]\right) \times$$
$$\times\, I_5(m_B^2, m_B^2, m_B^2, m_{\tilde{l}_{L2}}^2, m_{\tilde{l}_{R3}}^2) +$$
$$+ \left(\frac{m_\tau}{m_\mu}\left[-s_R^2 s_L c_L A_{\mu\tau}^R - s_R c_R s_L^2 A_{\mu\tau}^L +\right.\right.$$
$$\left. + s_R c_R s_L c_L \left(A_\tau + \frac{\mu_\rho \tan\gamma}{2}\right)\right] +$$
$$\left. + s_R^2 s_L^2 \left[A_\mu + \frac{\mu_\rho \tan\gamma}{2}\right]\right) \times$$
$$\left. \times\, I_5(m_B^2, m_B^2, m_B^2, m_{\tilde{l}_{L3}}^2, m_{\tilde{l}_{R3}}^2)\right], \quad (32)$$

where s_L, c_L and s_R, c_R are the mixing angles between flavor states $\tilde{\mu}_L$, $\tilde{\tau}_L$, $\tilde{\mu}_L^c$, $\tilde{\tau}_L^c$ and the mass states $\tilde{l}_{L2}$, $\tilde{l}_{L3}$, $\tilde{l}_{R2}$, $\tilde{l}_{R3}$:

$$\tilde{\mu}_L = c_L \tilde{l}_{L2} - s_L \tilde{l}_{L3}, \quad \tilde{\tau}_L = s_L \tilde{l}_{L2} + c_L \tilde{l}_{L3},$$

$$\tilde{\mu}_L^c = c_R \tilde{l}_{R2} - s_R \tilde{l}_{R3}, \quad \tilde{\tau}_L^c = s_R \tilde{l}_{R2} + c_R \tilde{l}_{R3}$$

with $c_L = \cos\theta_L$, $s_L = \sin\theta_L$, $c_R = \cos\theta_R$, $s_R = \sin\theta_R$. Also, A_μ and $A_{\mu\tau}^{L,R}$ are the respective couplings of smuon–smuon–neutral Higgs and smuon–stauon–neutral Higgs. More details can be found in [27].

7. NUMERICAL CALCULATION

The full parameter space of the SUSYE331 model contains dozens of parameters, but we can classify them into categories: the B/μ-term μ_ρ; the ratio of two vacua $\tan\gamma$; the gaugino masses m_B, m_λ; the right-handed slepton masses $m_{\tilde{l}_{R2}}$, $m_{\tilde{\nu}_{R2}}$, $m_{\tilde{l}_{R3}}$,$m_{\tilde{\nu}_{R3}}$; the left-handed slepton masses $m_{\tilde{l}_{L2}}$, $m_{\tilde{\nu}_{L2}}$, $m_{\tilde{l}_{L3}}$, $m_{\tilde{\nu}_{L3}}$; and the mixing terms A_μ, A_τ, $A^L_{\tau\mu}$, $A^R_{\tau\mu}$. To simplify the calculations, we can first make a rough estimation by taking the limit where $m_{\tilde{L}}$, m_B, m_λ, μ_ρ are equal to m_{SUSY}, and since A_τ and $A^{L,R}_{\mu\tau}$ are nondiagonal terms in the mixing matrix, which means that they are very small, we can approximate $A_\tau = A^{L,R}_{\mu\tau} = 0$.

In this limit, analytic expressions (28)–(32) can be written simply as

$$a^{(a)}_{\mu L} = -\frac{1}{18}\frac{g^2}{8\pi^2}\frac{m^2_\mu}{m^2_{SUSY}} + \frac{1}{54}\frac{1}{12}\frac{g'^2}{8\pi^2}\frac{m^2_\mu}{m^2_{SUSY}},$$

$$a^{(a)}_{\mu R} = \frac{1}{6}\frac{1}{12}\frac{g'^2}{8\pi^2}\frac{m^2_\mu}{m^2_{SUSY}},$$

$$a^{(b)}_{\mu L} = \frac{1}{12}\frac{g^2}{4\pi^2}\frac{m^2_\mu}{m^2_{SUSY}} + \frac{1}{4}\frac{g^2}{4\pi^2}\frac{m^2_\mu}{m^2_{SUSY}}\operatorname{sign}(\mu_\rho)\tan\gamma -$$
$$- \frac{1}{12}\frac{2}{3}\frac{g^2}{8\pi^2}\frac{m^2_\mu}{m^2_{SUSY}}(1+\operatorname{sign}(\mu_\rho)\tan\gamma) +$$
$$+ \frac{1}{12}\frac{4}{27}\frac{g'^2}{8\pi^2}\frac{m^2_\mu}{m^2_{SUSY}}(1+\operatorname{sign}(\mu_\rho)\tan\gamma),$$

$$a^{(b)}_{\mu R} = -\frac{1}{12}\frac{2}{9}\frac{g'^2}{8\pi^2}\frac{m^2_\mu}{m^2_{SUSY}}(1+\operatorname{sign}(\mu_\rho)\tan\gamma),$$

$$a^{(c)}_{\mu LR} = \frac{1}{12}\frac{1}{9}\frac{g'^2}{8\pi^2}\frac{m^2_\mu}{m^3_{SUSY}} \times$$
$$\times \operatorname{Re}\left[A_\mu + \frac{m_{SUSY}\operatorname{sign}(\mu_\rho)\tan\gamma}{2}\right].$$

If we assume that $A_\mu = 0$, then summing all the above terms gives

$$\Delta a^{total}_\mu = -\frac{1}{36}\frac{g^2}{8\pi^2}\frac{m^2_\mu}{m^2_{SUSY}} + \frac{1}{108}\frac{g'^2}{8\pi^2}\frac{m^2_\mu}{m^2_{SUSY}} +$$
$$+ \frac{4}{9}\frac{g^2}{8\pi^2}\operatorname{sign}(\mu_\rho)\tan\gamma\frac{m^2_\mu}{m^2_{SUSY}} +$$
$$+ \frac{1}{648}\frac{g'^2}{8\pi^2}\operatorname{sign}(\mu_\rho)\tan\gamma\frac{m^2_\mu}{m^2_{SUSY}}. \quad (33)$$

We first estimate Δa_μ numerically by using Eq. (33). From Eq. (33), we can conclude that Δa_μ has the same sign as μ_ρ. In Fig. 4, we plot the discrepancy of the muon MDM between experimental data and the SM prediction. For convenience, we scale the value of MDM by the factor 10^8 throughout in this paper. The shaded region is the 1.6σ difference with the upper and the lower bounds are 2.0σ–3.6σ. The muon MDM is investigated at different values $\tan\gamma = 1$, 5, 10, 20, 40, 60. We can see that to explain the $\geq 3.6\sigma$ difference, the mass of the supersymmetric particle can be as small as ≈ 75 GeV at $\tan\gamma = 1$. This is because the number of new particles is increased in the SUSYE331 model compared to the MSSM. Therefore, the contribution to the total value of the MDM is large even for small $\tan\gamma$. When $\tan\gamma$ is large ($\tan\gamma$=60), the mass of the SUSY particle m_{SUSY} is limited to 900 GeV in order to address the 2.0σ discrepancy. As pointed out in [21], the simple extension of the gauge symmetry model of the SM cannot address the MDM problem because of the damping term m^2_μ/M^2_{NP}, where M_{NP} is the mass of the new-physics particle. But in the supersymmetric version of the 3-3-1 model, the contribution of the new particle to the MDM is enhanced by a factor given by the ratio of two vacuum $\tan\gamma$. Therefore, the issue of the MDM can be addressed with a suitable value of $\tan\gamma$.

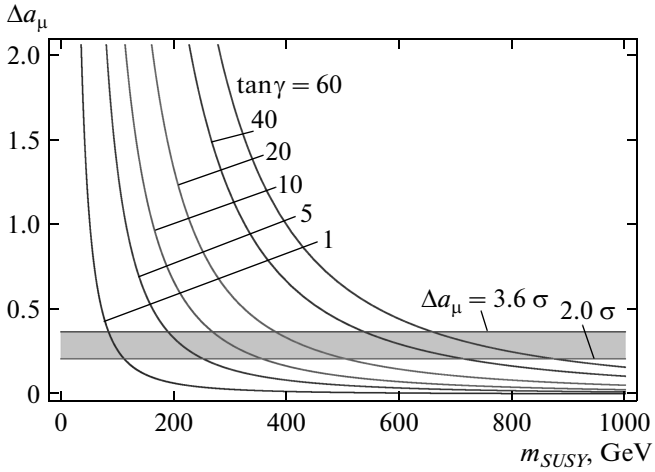

Fig. 4. Δa_μ plotted versus m_{SUSY}

Next, we obtain the SUSYE331 contribution to the muon MDM by using analytic expressions (28)–(32) and fixing the value of $\tan\gamma$ and slepton masses. We assume that $m_{\tilde{l}_2} = m_{\tilde{l}_{L2}} = m_{\tilde{l}_{R2}} = m_{\tilde{\nu}_{L2}} = m_{\tilde{\nu}_{R2}}$ and $m_{\tilde{l}_3} = m_{\tilde{l}_{L3}} = m_{\tilde{l}_{R3}} = m_{\tilde{\nu}_{L3}} = m_{\tilde{\nu}_{R3}}$. The mass hierarchy between the second and the third generation is taken into account. Since the MSSM is embedded in the SUSYE331, we can take the constraint on the smuon mass [1] where the smuon mass is greater than

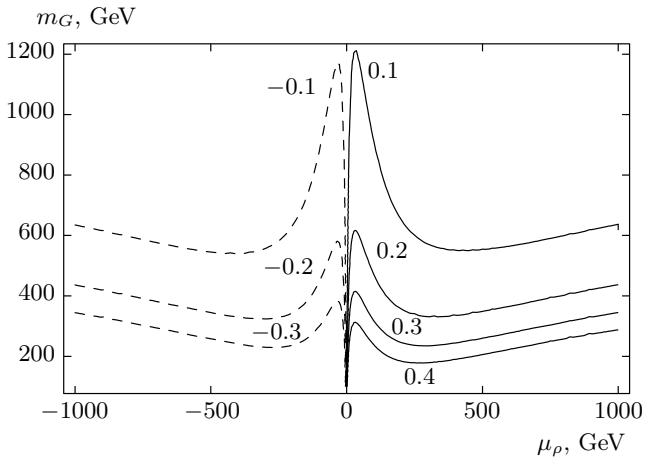

Fig. 5. Δa_μ plotted versus μ_ρ and m_G: $m_{\tilde{l}_2} = m_{\tilde{l}_{L2}} = m_{\tilde{l}_{R2}} = m_{\tilde{\nu}_{L2}} = m_{\tilde{\nu}_{R2}}$, $m_{\tilde{l}_3} = m_{\tilde{l}_{L3}} = m_{\tilde{l}_{R3}} = m_{\tilde{\nu}_{L3}} = m_{\tilde{\nu}_{R3}}$, $\tan\gamma = 5$, $m_{\tilde{l}_2} = 100$ GeV, $m_{\tilde{l}_3} = 1$ TeV, $m_B = m_\lambda = m_G$, $\theta_L = \theta_R = \pi/4$, $\theta_{\nu_L} = \theta_{\nu_R} = \pi/4$

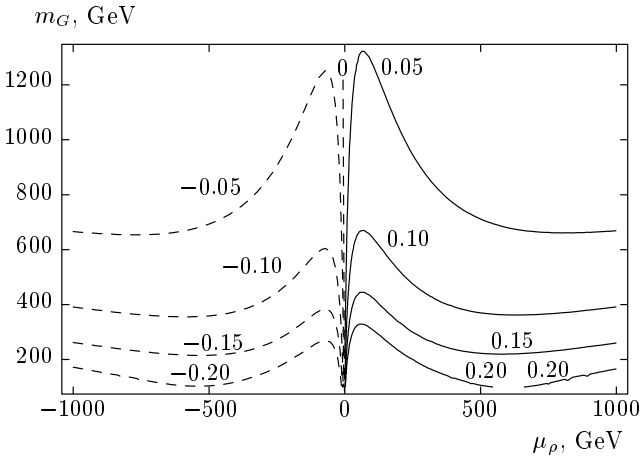

Fig. 6. Δa_μ plotted versus μ_ρ and m_G: $m_{\tilde{l}_2} = m_{\tilde{l}_{L2}} = m_{\tilde{l}_{R2}} = m_{\tilde{\nu}_{L2}} = m_{\tilde{\nu}_{R2}}$, $m_{\tilde{l}_3} = m_{\tilde{l}_{L3}} = m_{\tilde{l}_{R3}} = m_{\tilde{\nu}_{L3}} = m_{\tilde{\nu}_{R3}}$, $\tan\gamma = 5$, $m_{\tilde{l}_2} = 200$ GeV, $m_{\tilde{l}_3} = 1$ TeV, $m_B = m_\lambda = m_G$, $\theta_L = \theta_R = \pi/4$, $\theta_{\nu_L} = \theta_{\nu_R} = \pi/4$

91 GeV (ABBIENDI 04). We approximate the mass of the second generation as $m_{\tilde{l}_2} = 100$ GeV and in other cases as $m_{\tilde{l}_2} = 200$ GeV, while the third generation mass $m_{\tilde{l}_3}$ about 1 TeV. The results obtained in Fig. 4 show that if the SUSY masses are fixed in the range 100–200 GeV, the value of $\tan\gamma$ is 5 in order to fit the experimental results. Hence, we study the SUSY contribution to the muon MDM for fixed values of slepton masses and in the (m_G, μ_ρ) plane. In Figs. 5 and 6, we

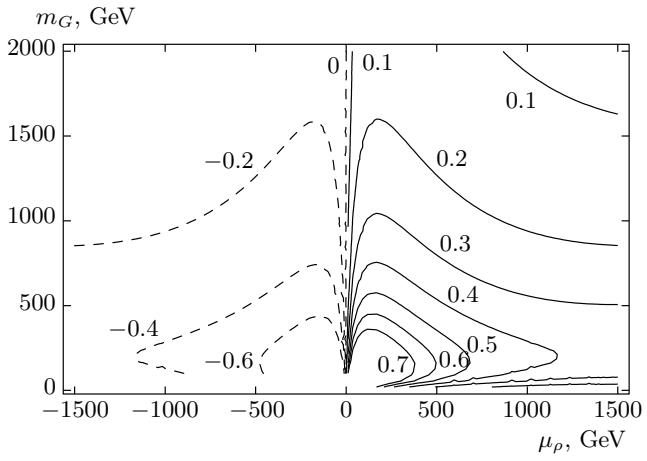

Fig. 7. Δa_μ plotted versus μ_ρ and m_G: $m_{\tilde{l}_2} = m_{\tilde{l}_{L2}} = m_{\tilde{l}_{R2}} = m_{\tilde{\nu}_{L2}} = m_{\tilde{\nu}_{R2}}$, $m_{\tilde{l}_3} = m_{\tilde{l}_{L3}} = m_{\tilde{l}_{R3}} = m_{\tilde{\nu}_{L3}} = m_{\tilde{\nu}_{R3}}$, $\tan\gamma = 60$, $m_{\tilde{l}_2} = 500$ GeV, $m_{\tilde{l}_3} = 2$ TeV, $m_B = m_\lambda = m_G$, $\theta_L = \theta_R = \pi/4$, $\theta_{\nu_L} = \theta_{\nu_R} = \pi/4$

plot the results for $\tan\gamma = 5$; the bino and gauginos masses are assumed to be equal to the gauginos mass, $m_B = m_\lambda = m_G$. The mixing is assumed maximal, $\theta_L = \theta_R = \pi/4$, $\theta_{\nu_L} = \theta_{\nu_R} = \pi/4$. The results given in Fig. 5 are plotted for $m_{\tilde{l}_2} = 100$ GeV and $m_{\tilde{l}_3} = 1$ TeV, while the results in the Fig. 6 are plotted for $m_{\tilde{l}_2} = 200$ GeV and $m_{\tilde{l}_3} = 1$ TeV. We plot for both negative and positive values of μ_ρ. There is a slight asymmetry in the graph caused by terms that do not depend on μ_ρ. We have imposed the condition of the maximum value of $|\mu_\rho| \leq 1500$ GeV to avoid fine-tuning requirement for the Higgs potential. We can see from Fig. 5 that in order to address the anomalous muon MDM data, the mass of the gauginos must be in the range $200 \leq m_G \leq 700$ GeV and because of the setup of the masses, $\tan\gamma = 5$ is the minimum value to satisfy the experimental discrepancy 2.0σ–3.6σ. We can also learn that the MDM value is inversely proportional to μ_ρ. In the case where the mass of the second generation is taken to be 200 GeV, Fig. 6, the MDM value merely reaches the 2.0σ anomaly of experimental data, which sets the upper bound on the second generation mass at 200 GeV for the mass of the third generation 1 TeV and $\tan\gamma = 5$. The results in Figs. 5 and 6 show that if we take a larger value of $m_{\tilde{l}_2}$, then the SUSYE331 contribution to the muon MDM is enhanced in the small m_G region.

We recall that the SUSYE331 contribution to the muon MDM is proportional to $\tan\gamma$. The results given in Fig. 4 show that if $\tan\gamma = 60$, then the interesting

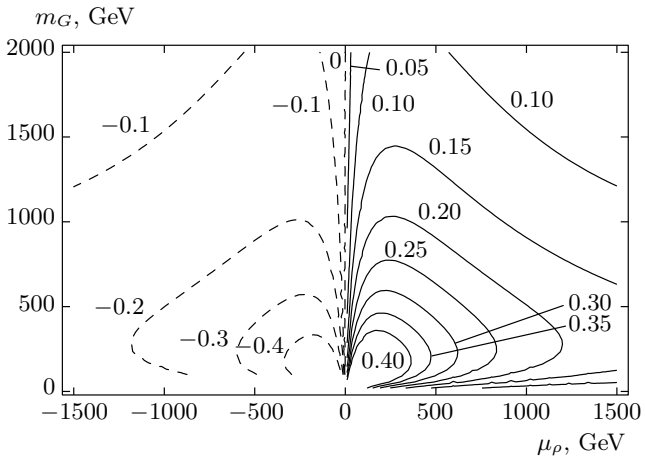

Fig. 8. Δa_μ plotted versus μ_ρ and m_G: $m_{\tilde{l}_2} = m_{\tilde{l}_{L2}} = m_{\tilde{l}_{R2}} = m_{\tilde{\nu}_{L2}} = m_{\tilde{\nu}_{R2}}$, $m_{\tilde{l}_3} = m_{\tilde{l}_{L3}} = m_{\tilde{l}_{R3}} = m_{\tilde{\nu}_{L3}} = m_{\tilde{\nu}_{R3}}$, $\tan\gamma = 60$, $m_{\tilde{l}_2} = 800$ GeV, $m_{\tilde{l}_3} = 2$ TeV, $m_B = m_\lambda = m_G$, $\theta_L = \theta_R = \pi/4$, $\theta_{\nu_L} = \theta_{\nu_R} = \pi/4$

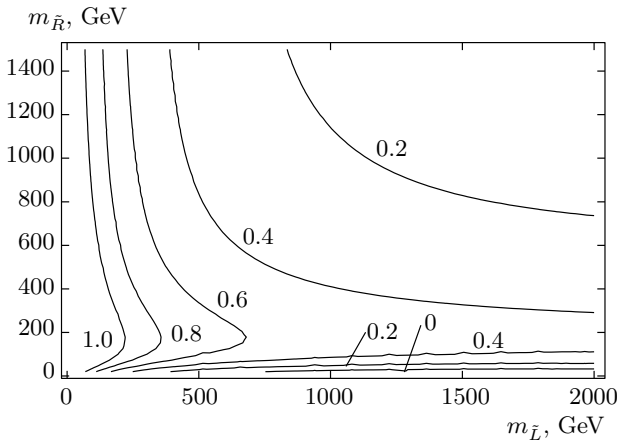

Fig. 9. Δa_μ plotted versus $m_{\tilde{L}}$ and $m_{\tilde{R}}$: $m_{\tilde{l}_{L2}} = m_{\tilde{\nu}_{L2}} = m_{\tilde{l}_{L3}} = m_{\tilde{\nu}_{L3}} = m_{\tilde{L}}$, $m_{\tilde{l}_{R2}} = m_{\tilde{\nu}_{R2}} = m_{\tilde{l}_{R3}} = m_{\tilde{\nu}_{R3}} = m_{\tilde{R}}$, $\tan\gamma = 60$, $\mu_\rho = 140$ GeV, $m_\lambda = 1$ TeV

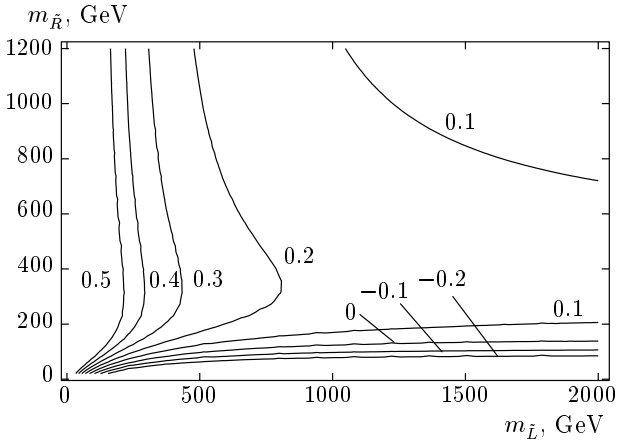

Fig. 10. Δa_μ plotted versus $m_{\tilde{L}}$ and $m_{\tilde{R}}$: $m_{\tilde{l}_{L2}} = m_{\tilde{\nu}_{L2}} = m_{\tilde{l}_{L3}} = m_{\tilde{\nu}_{L3}} = m_{\tilde{L}}$, $m_{\tilde{l}_{R2}} = m_{\tilde{\nu}_{R2}} = m_{\tilde{l}_{R3}} = m_{\tilde{\nu}_{R3}} = m_{\tilde{R}}$, $\tan\gamma = 60$, $\mu_\rho = 140$ GeV, $m_\lambda = 2$ TeV

m_{SUSY} region is 600–800 GeV. We impose the upper bound $\tan\gamma = 60$ (ACHARD 04) [1]. Hence, we numerically study the SUSYE331 contribution to the muon MDM in the case $\tan\gamma = 60$ and with the slepton mass hierarchy between the second and third family retained. In Figs. 7 and 8, we plot muon MDM on the (m_G, μ_ρ) plane with the same condition as above, but with the mass of the generation taken to be 500 GeV in Fig. 7 and 800 GeV in Fig. 8 and the mass of the third generation taken to be 2 TeV. The result in Fig. 7 show that the upper bounds $m_G = 1500$ GeV and $\mu_\rho = 1500$ GeV. However, the results in Fig. 8 set the upper bound $m_G = 1100$ GeV and $\mu_\rho = 1200$ GeV.

We next take into account the current upper bound on the Bino mass, 350 GeV, at the top quark mass 174 GeV based on the CP-violating phase [1]. We set $m_{\tilde{l}_{L2}} = m_{\tilde{\nu}_{L2}} = m_{\tilde{l}_{L3}} = m_{\tilde{\nu}_{L3}} = m_{\tilde{L}}$, $m_{\tilde{l}_{R2}} = m_{\tilde{\nu}_{R2}} = m_{\tilde{l}_{R3}} = m_{\tilde{\nu}_{R3}} = m_{\tilde{R}}$, and $\tan\gamma = 60$, $\mu_\rho = 140$ GeV. The mass of other gauginos m_λ is set to be 1 TeV (Fig. 9) and 2 TeV (Fig. 10). These figures illustrate the effects of varying $m_{\tilde{L}}$ and $m_{\tilde{R}}$ on the SUSYE331 contribution to the muon MDM. Combining the muon MDM from experiment and the theoretical predictions in (6) and (7), we obtain the relevant region of the parameter space. Especially, the region of the parameter space of $m_{\tilde{R}}$ is very large, $m_{\tilde{R}} > 20$ GeV, while that of $m_{\tilde{L}}$ is slightly constrained and depends on the value of the gaugino mass. If we fix $m_\lambda = 1$ TeV, the results given in Fig. 9 give the lower bound $m_{\tilde{L}} \approx 400$ GeV and there is no upper bound on $m_{\tilde{R}}$. From Fig. 10, we can find the upper bound on the left slepton mass $m_{\tilde{L}} \leq 800$ GeV.

Furthermore, by choosing the upper bound for the left-handed slepton mass above the third-generation masses $m_{\tilde{l}_{L3}} = m_{\tilde{l}_{R3}} = m_{\tilde{\nu}_{L3}} = m_{\tilde{\nu}_{R3}} = 800$ GeV and fixing $\tan\gamma = 60$, $\mu_\rho = 140$ GeV, and $m_B = 350$ GeV, we plot the SUSYE331 contribution to the muon MDM on the plane $(m_{\tilde{l}_{L2}} = m_{\tilde{\nu}_{L2}} = m_{L_2}$, $m_{\tilde{l}_{R2}} = m_{\tilde{\nu}_{R2}} = m_{R_2})$ in Fig. 11 and Fig. 12. The results in the cases $m_\lambda = 1$ TeV and $m_\lambda = 2$ TeV are shown in Fig. 11 and Fig. 12. Comparing with the experimental results, we find the lower bound $m_{L_2} > 500$ GeV for a fixed

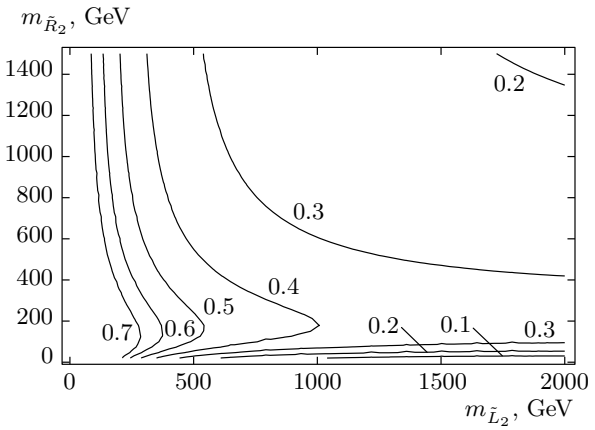

Fig. 11. Δa_μ plotted versus $m_{\tilde{L}_2}$ and $m_{\tilde{R}_2}$: $m_{\tilde{l}_{L2}} = m_{\tilde{\nu}_{L2}} = m_{L2}$, $m_{\tilde{l}_{R2}} = m_{\tilde{\nu}_{R2}} = m_{R2}$, $m_{\tilde{l}_{L3}} = m_{\tilde{l}_{R3}} = m_{\tilde{\nu}_{L3}} = m_{\tilde{\nu}_{R3}} = 800$ GeV, $\tan\gamma = 60$, $\mu_\rho = 140$ GeV, $m_B = 350$ GeV

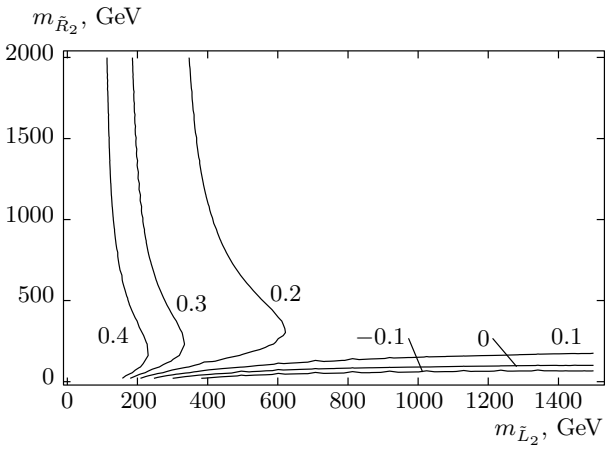

Fig. 12. Δa_μ plotted versus $m_{\tilde{L}_2}$ and $m_{\tilde{R}_2}$: $m_{\tilde{l}_{L2}} = m_{\tilde{\nu}_{L2}} = m_{L_2}$, $m_{\tilde{l}_{R2}} = m_{\tilde{\nu}_{R2}} = m_{R2}$, $m_{\tilde{l}_{L3}} = m_{\tilde{l}_{R3}} = m_{\tilde{\nu}_{L3}} = m_{\tilde{\nu}_{R3}} = 800$ GeV, $\tan\gamma = 60$, $\mu_\rho = 140$ GeV, $m_B = 350$ GeV

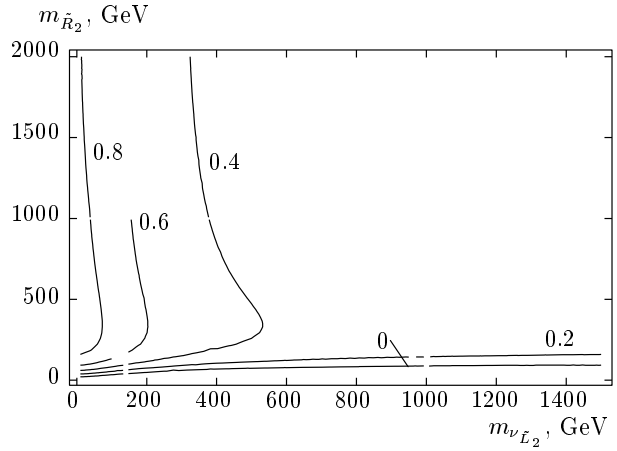

Fig. 13. Δa_μ plotted versus $m_{\tilde{\nu}_{L2}}$ and $m_{\tilde{R}_2}$: $\theta_R = \theta_L = 0$ and $\theta_{\nu_R} = \theta_{\nu_L} = \pi/4$, $\tan\gamma = 60$, $\mu_\rho = 140$ GeV, $m_{R3} = 800$ GeV, $m_{\tilde{L}_2} = 600$ GeV, $m_B = 350$ GeV, $m_\lambda = 1$ TeV

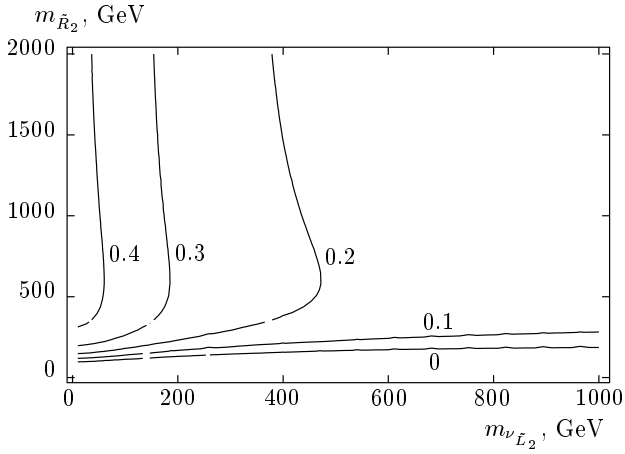

Fig. 14. Δa_μ plotted versus $m_{\tilde{\nu}_{L2}}$ and $m_{\tilde{R}_2}$: $\theta_R = \theta_L = 0$ and $\theta_{\nu_R} = \theta_{\nu_L} = \pi/4$, $\tan\gamma = 60$, $\mu_\rho = 140$ GeV, $m_{R_3} = 800$ GeV, $m_{\tilde{L}_2} = 600$ GeV, $m_B = 350$ GeV, $m_\lambda = 2$ TeV

$m_\lambda = 1$ TeV and the upper bound on the mass of the left-handed slepton of the second generation is 600 GeV for a fixed $m_\lambda = 2$ TeV. There is no bound on the right-handed slepton mass of the second generation.

We have investigated the maximal mixing case, where $\theta_{\nu_R} = \theta_{\nu_L} = \pi/4$ are related to the neutrino mixing and $\theta_R = \theta_L = \pi/4$ are related to the charged lepton mixing. Next, we investigate the case of smaller $\theta_R = \theta_L = 0$ and $\theta_{\nu_R} = \theta_{\nu_L} = \pi/4$. In Figs. 13 and 14, we plot the MDM dependence on the $m_{\tilde{\nu}_{L2}}$ and m_{R_2}, where we use the above constraint $m_{\tilde{L}_2} = 600$ GeV and other parameters are fixed as $\tan\gamma = 60$, $\mu_\rho = 140$ GeV, $m_{R_3} = 800$ GeV, $m_B = 350$ GeV, and $m_\lambda = 1$ TeV for Fig. 13 and $m_\lambda = 2$ TeV for Fig. 14. The sneutrino mass has to be smaller than 550 GeV to address the 2.0σ–3.6σ discrepancy if $m_\lambda = 2$ TeV. The lower bound of the right-handed slepton mass of the second generation is around tens of GeV for a fixed $m_\lambda = 1$ TeV and is a hundred GeV for a fixed $m_\lambda = 2$ TeV.

8. CONCLUSIONS

We have examined the muon $g-2$ in detail in the framework of the SUSYE331 model. We calculated

one-loop SUSYE331 contributions to the muon MDM based on both the mass eigenstate and the weak eigenstate methods. The mass eigenstates of the neutralino and chargino are obtained using an approximate method. To recognize the effects of the SUSYE331 parameters on the muon MDM, we work with analytic expressions of the muon MDM based on the mass insertion method. We have considered all parameters of SUSYE331 as free parameters. In our calculation we have made some assumptions: the maximal mixing and small mixing terms A_τ, A_μ, and $A^{L,R}_{\mu\tau}$, which are neglected in our calculation. In particular, by taking the limit where μ_ρ, m_λ, $m_{\bar{L}}$, m_B are equal to m_{SUSY}, we obtain reduced analytic expressions for the contribution of the SUSYE331 to the muon MDM. The results show that the SUSYE331 contribution to the muon MDM is enhanced in the small region of m_{SUSY} and large values of $\tan\gamma$. We have investigated for both small and large values of the ratio of two vacuum $\tan\gamma$ values. The numerical results show that consistency with the experimental bound on the muon MDM requires that $m_{SUSY} \approx 75$ GeV for $\tan\gamma = 1$ and $m_{SUSY} = 900$ for $\tan\gamma = 60$. On the other hand, we also investigated the SUSYE31 contribution to the muon MDM in the case of the mass hierarchy between the second and third generations. In the case where $\tan\gamma$ is small ($\tan\gamma = 5$) and one generation of the slepton mass is fixed at $\mathcal{O}(1)$ TeV, the light slepton particle mass is bounded from 100 GeV to 200 GeV and Δa^μ can be comparable to the current limit on the muon MDM. When $\tan\gamma$ is large ($\tan\gamma = 60$), the mass of the light left-handed slepton particle is bounded by 800 GeV. Finally, we note that in the case of the maximal flavor mixing only in the sneutrino sector, we obtain that the upper bound of the sneutrino mass is 550 GeV. These values can be examined at the LHC or the future collider ILC.

D. T. Binh thanks Le Tho Hue for his suggestion. This research is funded by the Vietnam National Foundation for Science and Technology Development (NAFOSTED) under the grant No. 103.01-2014.51.

APPENDIX

In this section, we define some integrals used in our calculation. The following integral is defined in [34]:

$$I^{(N)}(\nu_i;\nu_j) \equiv \int \frac{d^D k}{(k^2-m_1^2)^{\nu_1}\dots(k^2-m_N^2)^{\nu_N}} = \int \frac{d^D k}{\Pi_{j=1}^N (k^2-m_j^2)^{\nu_j}}.$$

In the special case where $D = 4$ and there are two masses, we have

$$I^{(2)}(\nu_1,\nu_2;m_1,m_2) = \pi^2 i^{-3}(-m_2)^{2-\nu_1-\nu_2} \times \times \frac{\Gamma(\nu_1+\nu_2-2)}{\Gamma(\nu_1+\nu_2)} \times \times {}_2F_1\left(\nu_1+\nu_2-2,\nu_1;\nu_1+\nu_2;1-\frac{m_1^2}{m_2^2}\right).$$

The loop integrals are defined as

$$I_N(m_1^2,\dots,m_N^2) = \frac{i}{\pi^2}\int \frac{d^4k}{(k_1^2-m_1^2)\dots(k_1^2-m_N^2)},$$

$$J_N(m_1^2,\dots,m_N^2) = \frac{i}{\pi^2}\int \frac{k^2 d^4k}{(k_1^2-m_1^2)\dots(k_1^2-m_N^2)}.$$

REFERENCES

1. J. Beringer et al., (Particle Data Group), Phys. Rev. D **86**, 010001 (2012).
2. H. N. Long, Phys. Rev. D **54**, 4691 (1996).
3. F. Pisano, V. Pleitez, Phys. Rev. D **46**, 410 (1992).
4. R. Foot, H. N. Long, and T. A. Tran, Phys. Rev. D **50**, R34 (1994).
5. C. A. de S. Pires and P. S. Rodrigues da Silva, JCAP **012**, 0712 (2007).
6. J. K. Mizukoshi, C. A. de S. Pires, F. S. Queiroz, and P. S. R. da Silva, Phys. Rev. D **83**, 065024 (2011).
7. F. Queiroz, C. A. de S. Pires, and P. S. R. da Silva, Phys. Rev. D **82**, 065018 (2010).
8. D. Cogollo, A. V. de Andrade, F. S. Queiroz, and P. R. Teles, Eur. Phys. J. C **72**, 2029 (2012).
9. J. D. Ruiz-Alvarez, C. A. de S. Pires, F. S. Queiroz, D. Restrepo, and P. S. Rodrigues da Silva, Phys. Rev. D **86**, 075011 (2012).
10. P. V. Dong, H. N. Long, and H. T. Hung, Phys. Rev. D **86**, 033002 (2012).
11. A. Alves, E. R. Barreto, A. G. Dias, C. A. de S. Pires, F. S. Queiroz, and P. S. Rodrigues da Silva, Eur. Phys. J. C **73**, 2288 (2013).
12. P. V. Dong, H. T. Hung, and T. D. Tham, Phys. Rev. D **87**, 115003 (2013).
13. P. V. Dong, T. Phong Nguyen, and D. V. Soa, Phys. Rev. D **88**, 095014 (2013).

14. P. V. Dong, H. N. Long, D. T. Nhung, and D. V. Soa, Phys. Rev. D **73**, 035004 (2006).

15. D. T. Huong, P. V. Dong, C. S. Kim, and N. T. Thuy, Phys. Rev. D **91**, 055023 (2015); P. V. Dong, D. T. Huong, F. S. Queiroz, and N. T. Thuy, Phys. Rev. D **90**, 075021 (2014).

16. C. A. de S. Pires and P. S. Rodrigues da Silva, Phys. Rev. D **64**, 117701 (2001).

17. C. A. De Sousa Pires and P. S. Rodrigues da Silva, Phys. Rev. D **65**, 076011 (2002).

18. N. A. Ky, H. N. Long, and D. V. Soa, Phys. Lett. B **486**, 140 (2000).

19. C. Kelso, P. R. D. Pinheiro, F. S. Queiroz, and W. Shepherd, Eur. Phys. J. C **74**, 2808 (2014).

20. C. Kelso, H. N. Long, R. Martinez, and F. S. Queiroz, Phys. Rev. D **90**, 113011 (2014).

21. A. Czarnecki and W. J. Marciano, Phys. Rev. D **64**, 013014 (2001).

22. M. J. G. Veltman, Acta Phys. Pol. B **12**, 437 (1981).

23. P. Langacker and M. Luo, Phys. Rev. D **44**, 817 (1991).

24. P. Fayet, in *Unification of the Fundamental Particles Interactions*, ed. by S. Ferrara, J. Ellis, and P. van Nierwenhuizen, Plenum, New York (1980), p. 587; J. A. Grifols and A. Mendez, Phys. Rev. D **26**, 1809 (1982); J. Ellis, J. S. Hagelin, and D. V. Nanopoulos, Phys. Lett. B **166**, 283 (1982); R. Barbieri and L. Maiani, Phys. Lett. B **117**, 203 (1982); D. A. Kosower, L. M. Krauss, and N. Sakai, Phys. Lett. B **133**, 305 (1983); T. C. Yuan, R. Arnowitt, A. H. Chamseddine, and P. Nath, Z. Phys. C **26**, 407 (1984); J. C. Romao, A. Barroso, M. C. Bento, and G. C. Branco, Nucl. Phys. B **250**, 295 (1985); J. Lopez, D. V. Nanopoulos, and X. Wang, Phys. Rev. D **49**, 366 (1991); U. Chattopadhyay and P. Nath, Phys. Rev. D **53**, 1648 (1996); T. Moroi, Phys. Rev. D **53**, 6565 (1996).

25. J. Ellis and D. V. Nanopoulos, Phys. Lett. B **110**, 44 (1982); I.-H. Lee, Phys. Lett. B **138**, 121 (1984); Nucl. Phys. B **246**, 120 (1984).

26. P. V. Dong, D. T. Huong, M. C. Rodriguez, and H. N. Long, Nucl. Phys. B **772**, 150 (2007).

27. P. T. Giang, L. T. Hue, D. T. Huong, and H. N. Long, Nucl. Phys. B **864**, 85 (2012).

28. L. T. Hue, D. T. Huong, and H. N. Long, Nucl. Phys. B **873**, 207 (2013).

29. A. Brignole and A. Rossi, Nucl. Phys. B **701**(3), 53 (2004); K. S. Babu and C. Kolda, Phys. Rev. Lett. **89**, 241802 (2002); A. Abada, D. Das, and C. Weiland, JHEP **1203**, 100 (2012); A. Abada, D. Das, A. Vicent, and C. Weiland, JHEP **1209**, 015 (2012).

30. D. T. Huong and H. N. Long, JHEP **049**, 0807 (2008).

31. P. V. Dong, Tr. T. Huong, N. T. Thuy, and H. N. Long, JHEP **073**, 0711 (2007).

32. M. Davier et al., Eur. Phys. J. C **66**, 127 (2010); A. Hoecker, B. Malaescu, C. Z. Yuan, and Z. Zhang, Eur. Phys. C **66**, 1 (2010).

33. Muon G-2 Collaboration, Phys. Rev. D **73** (2006).

34. A. I. Davydychev, J. Math. Phys. **32**, 4299 (1991).